Journal of
Materials Chemistry B

PAPER

View Article Online
View Journal | View Issue

Cite this: *J. Mater. Chem. B*, 2015, 3, 2954

Sensing cell adhesion using polydiacetylene-containing peptide amphiphile fibres†

B. E. I. Ramakers,‡ S. A. Bode,‡ A. R. Killaars, J. C. M. van Hest and D. W. P. M. Löwik*

Received 19th December 2014,
Accepted 20th February 2015

DOI: 10.1039/c4tb02099e

www.rsc.org/MaterialsB

Sensing cell adhesion by means of a colourimetric response provides an intuitive measure of cell binding. In this study polydiacetylene-containing peptide amphiphiles fibres were designed to sense cell adhesion by means of a colour change. The diacetylene-containing peptide amphiphiles were functionalised with the cell-binding motif RGDS, and subsequently mixed with non-functionalised diacetylene-containing spacer amphiphiles. The diacetylenes in the backbone of these fibres were polymerised using UV-light to give dark blue fibre solutions. Subsequent cell adhesion induced a colour change from blue to pink. The propensity of the RGDS fibres to change colour upon cell adhesion could be tuned by varying the C-terminal amino acid of the spacer amphiphile. In addition to this, by varying the RGDS density we found that the optimum colourimetric response was obtained for fibres with a 6 : 1 ratio of non-RGDS to RGDS amphiphiles.

Introduction

Polydiacetylenes are an interesting class of conjugated polymers with intrinsic optical properties. In addition to absorbing light in the visible region they can undergo a colour change in response to external stimuli, which makes them promising molecular probes for sensing their environment.[1–3] Polydiacetylenes can be easily prepared through topochemical polymerisation of the diacetylene monomers using ultraviolet (UV) irradiation.[4] However, their formation is subject to the distance between the monomers and the angle between the moieties, which must be ~4.9 Å and ~45° respectively.[5] Systems in which these requirements are met include fibres,[6–8] monolayers,[9–11] and vesicles[12,13] Charych *et al.* were first to utilize the sensing properties of polydiacetylenes by decorating polydiacetylene-based liposomes with sialic acid and monitoring the colour change of the polydiacetylene backbone upon addition of the influenza virus.[14] They found that the ultraviolet-visible (UV-Vis) spectrum of the liposomes shifted from ~630 nm to ~490 nm, which coincides with a colour change from blue to red upon binding of the virus. Since then various polydiacetylene-based sensors have been designed to detect a wide variety of analytes such as microorganisms,[15,16] various proteins,[17–19] and even membrane perturbing events in cells.[20,21] In these sensor systems the polydiacetylene was incorporated in coatings, vesicles or liposomes. Polydiacetylene formation has also been realized in well-organised peptide amphiphile fibres, as a means of creating disassembly-resistant architectures, but not to exploit their colourimetric properties. In one example, Stupp and co-workers functionalised the peptide Lys-Lys-Leu-Leu-Ala-Lys with a diacetylene-containing alkyl tail and found that these amphiphilic molecules could self-assemble into fibres.[6] Furthermore, the diacetylenes could then be cross-linked using UV-light to yield fibres with an intense blue colour which is indicative of polydiacetylene formation. In similar work, polymerised fibres were prepared from a diacetylene-containing alkyl tail coupled to a peptide segment based on the circumsporozoite (CS) protein of a malaria parasite.[8,22,23]

These peptide-based materials can be efficiently tailored with to induce biological function, for example to facilitate cell adhesion. The RGD domain is probably the most applied cell adhesion motif, and as such has been introduced onto numerous materials.[24–33]

An example includes the peptide amphiphile fibres used by Webber *et al.* to culture bone-marrow mononuclear cells.[34] However, the alkyl tail in these fibres did not contain a diacetylene functionality. A two-dimensional polydiacetylene based material was used for cell culture by Biesalski and co-workers. They synthesised amphiphiles composed of a 10,12-tricosadiynoic acid tail and a

Radboud University Nijmegen, Institute for Molecules and Materials, Bio-organic Chemistry, Heyendaalseweg 135, 6525 AJ Nijmegen, The Netherlands. E-mail: d.lowik@science.ru.nl

† Electronic supplementary information (ESI) available: Materials and detailed experimental procedures for cell culture, integrin binding, liquid chromatography mass spectroscopy, reversed phase HPLC, chromatic ratio calculations, temperature dependent UV-Vis absorption spectra and transmission electron microscopy can be found in the supporting information. ESI figures include transmission electron micrographs, UV-Vis spectra used to calculate chromatic ratios, absorption *vs.* temperature graphs used to calculate the transition temperature, brightfield micrographs, confocal laser scanning micrographs, HPLC traces. See DOI: 10.1039/c4tb02099e

‡ Equal contribution.

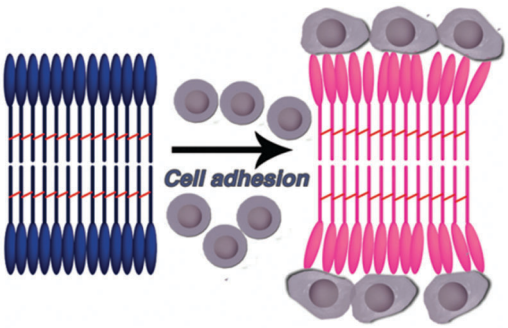

Fig. 1 Schematic representation of the concept of a cell-adhesion induced colourimetric response.

GRGDSP head group.[9] They were able to use diacetylenes to cross-link monolayers comprised of these peptide amphiphiles. In this example the polydiacetylene functionality was again only used to stabilise the monolayers. Until now, the sensory properties of polydiacetylenes have not been employed in conjunction with any type of cell binding scaffold to detect the interaction with mammalian cells. This would be a valuable feature as it would allow a direct visualization of the adhesion process and also could be used to study cell migration in materials by visual inspection.

In this study we report to the best of our knowledge, for the first time, polydiacetylene-containing peptide amphiphile fibres that have the right level of stability to be used as a sensitive colourimetric sensor for cell adhesion (Fig. 1). To achieve this we functionalised diacetylene-containing peptide amphiphiles with the cell adhesion motif RGDS and mixed these with spacer (non-RGDS) diacetylene-containing amphiphiles to form nanofibres. We found that the propensity of the RGDS fibres to change colour in response to cell adhesion could be tuned by varying the C-terminal amino acid of the spacer amphiphiles. It was found that the degree of the colour change was related to the amount of RGDS amphiphile present in the fibre.

Experimental

Synthesis of peptide amphiphiles

PA 1 was synthesised from 1 g of 2-chlorotrityl resin (1 mmol g^{-1}). The resin was swollen in dry dichloromethane (DCM). 2 equivalents of the relevant amino acid and 3 equivalents of diisopropylethylamine (DiPEA) were dissolved in dry DCM and added to the resin. Subsequent couplings were carried out with 3.0 equivalents of the required amino acid, 3.3 equivalents of DIPCDI and 3.6 equivalents of 1-hydroxybenzotriazole hydrate (HOBt) in dimethylformamide (DMF), and all deprotections were achieved with 20% piperidine in DMF. After each coupling and deprotection a Kaiser test was used to ensure the reaction had gone to completion.[35] Finally 10,12-pentacosadiynoic acid was coupled to the peptide using 3 equivalents of the acid, 3.3 equivalents of DIPCDI and 3.6 equivalents of HOBt. The peptide was cleaved from the resin by treatment of the resin with a mixture of trifluoroacetic acid (TFA)/triisopropylsilane (TIS)/H_2O (95 : 2.5 : 2.5) for 3 hours, followed by precipitation in ether or by removal of the solvents under reduced pressure. The peptides were lyophilised from acetic acid and purified using preparative HPLC. The peptides were characterised using analytical HPLC and LCMS.

Fibre preparation

The peptide amphiphiles were dissolved in PBS (140 mM NaCl, 2.6 mM KCl, 1.5 mM KH_2PO_4, 10 mM Na_2HPO_4, pH 7.2) at concentrations of 1.0 mg mL^{-1}. The samples were sonicated for 15 minutes at 25 °C, subsequently heated to 90 °C and allowed to cool to room temperature in the water bath overnight. For the fibres with a C-terminal Asp and Glu, the samples were prepared at 2.0 mg mL^{-1} as described above and diluted with 2× PBS to give a final fibre concentration of 1.0 mg mL^{-1}.

Polymerisation

Polymerisations were carried out on 1.0 mg mL^{-1} samples in a 4 mL glass vial (containing approximately 1.5 mL fibre solution), which was open and illuminated from above using a Bluepoint 2 UV lamp with a lamp–sample distance of 3 cm for 999 s.

Brightfield microscopy

Fibre solutions (1 mg mL^{-1} in PBS) were prepared as previously mentioned. To each well of an 8-chambered coverslip (Nunc, Wiesbaden, Germany) 150 μL of the fibre solution was added. Then, 40 000 HeLa cells in 150 μL phenol-red free Dulbecco Modified Eagle Medium (DMEM) + 10% Fetal Bovine Serum (FBS) were seeded in each well. Wells coated with gelatin were used as a control sample and these were prepared by incubating the wells with a 0.1% gelatin solution for 15 minutes, after which the excess gelatin was removed. In these control wells, 40 000 HeLa cells were seeded in 300 μL phenol-red free DMEM + 10% FBS. The cells were then incubated for 18 hours at 37 °C/7.5% CO_2. After the incubation period, the colour of the samples and the cell adhesion to the fibres was analysed by brightfield microscopy. For these experiments, the white balance of the brightfield camera was set using the transparent gelatin controls. These controls were furthermore used to verify the quality of the samples. All images in one experiment were recorded using the same camera settings.

UV-Vis spectroscopy after incubation with cells

Fibre solutions (1 mg mL^{-1} in PBS) were prepared as previously mentioned. For this experiment, 48-well plates were used. In each well, 175 μL of the fibre solution was added. Then, 60 000 HeLa cells in 175 μL phenol-red free DMEM + 10% FBS were mixed in with the fibre solutions in each well. As a control to verify the quality of the sample, wells were coated with a 0.1% gelatin solution for 15 minutes, after which the excess gelatin was removed. In these control wells, 60 000 HeLa cells were seeded in 350 μL phenol-red free DMEM + 10% FBS. The cells were then incubated for 18 hours at 37 °C/7.5% CO_2. After the incubation period, the samples were transferred to a cuvette and measured by UV-Vis absorption spectroscopy. UV-Vis spectra of the fibre samples with/without cells were recorded on a Varian Cary-50 spectrometer using a 1 mm quartz cuvette. For each sample

the chromatic ratio was calculated using the absorptions at 634 nm (A_{blue}) and 558 nm (A_{red}). Chromatic ratios (CR) were calculated using the following equation:[14] CR = [PB0 − PB1/PB0]·100, where PB0 = pre-exposure to analyte and PB1 = post-exposure to analyte. PB = $A_{blue}/(A_{blue} + A_{red})$

Cell viability

For the cell viability experiments, the samples were prepared similarly to the brightfield microscopy samples. Only after the incubation period of 18 hours at 37 °C/7.5% CO_2, the cells were treated with the live/dead staining, which was prepared by diluting calcein AM and ethidium homodimer-1 (EthD-1) in PBS to obtain a concentration of 8 μM calcein AM and 16 μM EthD-1. To each well, 100 μL of the staining solution was added, yielding a final concentration of 2 μM calcein AM and 4 μM EthD-1. The samples were then allowed to rest for 10 minutes, after which they were immediately analysed by confocal laser scanning microscopy. Calcein was excited with the 488 nm line of an argon ion laser, and emission was collected between 494 and 515 nm. EthD-1 was excited with the 561 nm line of a yellow diode laser and emission was collected between 600 and 625 nm. Using the ImageJ software, overlay images of the calcein and EthD-1 signals were produced. The overlay images can be found together with their corresponding transmission images in Fig. S2.5 (ESI†). For the series of K-fibres (3 : 1, 6 : 1, 12 : 1, 24 : 1, scrambled and spacer K-fibres) the total amount of cells (living and dead) was counted for each sample (composed of at least 4 images for each sample) and from this the average total amount of cells could be calculated (Fig. 4B). Next, the average total amount of living, spread cells was counted for each sample (data obtained from the same images as used to calculate the average total amount of cells). This was then used to calculate the ratio between spread cells and the total amount of cells (Fig. 4B). The optimal concentrations for the live/dead dyes were determined by staining dead HeLa cells with a varying concentration of EthD-1 (between 1 and 10 μM). From this, it was found that at a concentration of 4 μM EthD-1 the nuclei were brightly fluorescing, whereas the cytoplasm was not stained. Similarly, the optimal concentration of calcein AM was determined by treating dead HeLa cells with a ranging concentration of 1 to 10 μM calcein AM to avoid aspecific staining of the cytoplasm. The best results were obtained using concentrations lower than 2 μM. We then verified that this concentration gave sufficient fluorescence in living HeLa cells.

Results and discussion

The structural part of the peptide amphiphiles was designed to contain two components, the hydrophilic peptide sequence found in silk-worm silk, containing repeating glycine and alanine residues, and a 10,12-pentacosadiynoic acid alkyl tail.[36–38] In this way the formation of stable fibres was enabled as a result of both the hydrophobic interactions of the alkyl tails and the β-sheet-forming character of the peptides. By manipulating the C-terminal amino acid of the spacer amphiphile (C_{25}Gly-Ala-Gly-Ala-Xaa), we aimed to tune the stability of the fibres and thus the susceptibility of the polydiacetylene backbone to colour change (Fig. 2A). Previous studies have shown that the amino acid sequence of the peptide segment in these fibres can have a marked effect on the sensitivity of the diacetylene backbone to environmental changes.[11,39] In order to allow for cell adhesion on the surface of the fibres we synthesised an amphiphile with the sequence $^{10,12}C_{25}$-Gly-Ala-Gly-Ala-Lys-Arg-Gly-Asp-Ser (RGDS amphiphile) and as a control an amphiphile with the scrambled cell adhesion sequence $^{10,12}C_{25}$-Gly-Ala-Gly-Ala-Lys-Asp-Gly-Ser-Arg (scrambled amphiphile) (Fig. 2A). In order to obtain tuneable nanofibres with respect to composition, a spacer amphiphile was mixed with the RGDS amphiphile or scrambled amphiphile. The first letter of the fibre name indicated the amino acid at the C-terminal position of the spacer amphiphile. In this way we aimed to create an RGDS-containing fibre that was stable enough to resist changing colour at the conditions required for cell growth but sensitive enough to change colour due to cell adhesion on the surface of the fibres.

For the fibre solutions to be compatible with cell growth, polydiacetylene fibre formation should be possible in phosphate buffer saline (PBS). All of the spacer amphiphiles were able to form fibres in PBS with the exception of the E-spacer and D-spacer amphiphiles which were first formed in water and diluted with concentrated PBS. Both of the E- and D-spacer fibre solutions became dark purple and slightly aggregated upon the addition of PBS. The structure of the various fibres was investigated using transmission electron microscopy (TEM) (Fig. 2C and Fig. S2.1, ESI†). All the fibres had a similar ribbon-like morphology, with the exception of fibres consisting of the K-spacer amphiphile in which small aggregates comprised of short fibres were observed in addition to extended fibres.

Inspired by the results obtained by Stupp and co-workers we initially chose to mix the spacer amphiphile and RGDS amphiphile or scrambled amphiphile in a ratio of 6 : 1 respectively (Fig. 2B).[34] Subsequently, we investigated the susceptibility to colour change of the polydiacetylene backbone in the RGDS-containing fibres with respect to increasing temperature. We found that merely varying the C-terminal amino acid of the spacer amphiphile had a marked effect on the temperature at which a colour change occurred in the fibres. The E-RGDS fibres were most sensitive to a temperature induced colour change, changing colour at 37 °C, whereas the A-RGDS fibres were most temperature stable, only exhibiting a colour change at 53 °C (Fig. 2D). The RGDS fibres based on the remaining spacer amphiphiles exhibited a temperature induced colour change at temperatures spanning this range (Fig. 2D). The temperature at which the fibres exhibit a colour change does not correlate directly with the β-sheet forming propensity of the C-terminal amino acid, which suggests it occurs as a result of more subtle effects.[40] The fact that the different RGDS-containing fibres changed colour at different temperatures also suggests that the colour change due to cell adhesion will be more pronounced in some fibres than in others, and thus that the choice of spacer amphiphile is a crucial element in the overall design of the sensor. With this library of peptide fibres in hand, we were able to test the ability of HeLa cells to adhere

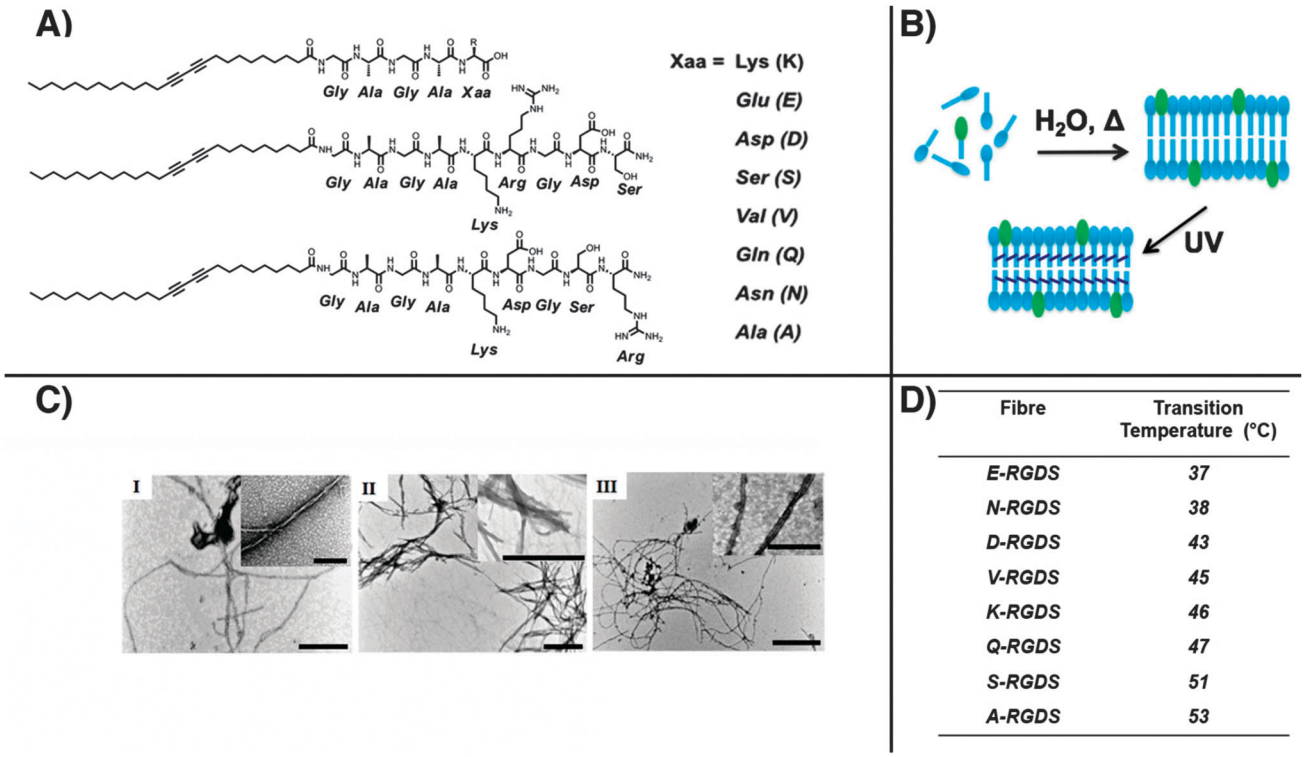

Fibre	Transition Temperature (°C)
E-RGDS	37
N-RGDS	38
D-RGDS	43
V-RGDS	45
K-RGDS	46
Q-RGDS	47
S-RGDS	51
A-RGDS	53

Fig. 2 (A) The structures of the amphiphiles used in this study. (B) Schematic representation of the assembly of RGDS-fibres in water and the polymerisation using UV light to cross-link the amphiphiles. The spacer amphiphiles are shown in blue and the RGDS amphiphiles are shown in green. The first letter of the fibre name indicates the amino acid at the C-terminal position of the spacer amphiphile. (C) Transmission electron micrographs of the fibres (I) E-fibres, scale bars represent 500 nm and 200 nm (magnification) (II) K-fibres, scale bars represent 2 μm and 500 nm (magnification) (III) A-fibres, scale bars represent 2 μm and 200 nm (magnification) (D) table showing the transition temperatures of the various RGDS-fibres composed of a 6 : 1 ratio of spacer amphiphile to RGDS amphiphile.

to their surface and investigate the effect of cell adhesion on the colour of the polydiacetylene backbone of the fibres. We performed brightfield microscopy on living cells which not only allowed the analysis of the colour of the sample, but also provided information about the cell morphology (Fig. 3A). The samples were prepared by mixing detached HeLa cells (40 000 per sample) in phenol-red free culture medium with the fibre solutions so that a concentration of 0.5 mg mL^{-1} of the fibres was obtained. Phenol-red free culture medium was used so that a potential colour change could be clearly visualised. The mixture of HeLa cells and fibres was then seeded in 8-well chambered microscopy slides. The cells were incubated for 18 hours at 37 °C. For each experiment, a positive control was carried out by seeding 40 000 HeLa cells onto a gelatin-coated chamber of the microscopy slides. Furthermore, negative controls were performed using fibres that were not functionalised with RGDS (spacer fibres) as well as fibres that contained the amphiphiles with the scrambled cell adhesion sequence DGSR (Fig. 2A). In order to be able to determine the extent of the colour change more accurately, control samples without cells were prepared for every experiment. These samples were treated in the same manner as the samples with cells. To ensure that the buffer, fibre and serum concentrations in these samples were the same as in the samples containing cells, the sample preparation was performed by mixing the fibre solution with an equal amount of phenol-red free medium supplemented with 10% FBS. After the incubation period, all samples were immediately studied using brightfield widefield microscopy.

The gelatin control was used to verify the quality of the samples and to set the white-balance for the brightfield camera. These experiments showed that in general RGDS-fibres promoted cell adhesion, giving rise to nicely spread cells, and this observation was independent of the type of spacer amphiphile in the fibres. There were three exceptions, in both the Q-RGDS and the N-RGDS samples the cell count was severely reduced and a similar effect was seen for the D-RGDS fibres, although in this case the effect was less pronounced (see ESI,† Fig. S2.4.2 and S2.5.2).

With respect to the colourimetric properties, only the K-RGDS-fibres showed a colour change from blue to pink upon cell adhesion and importantly, both the spacer and scrambled fibre samples retained their original blue colour. As was expected from the temperature UV-Vis data, the E-fibres already changed colour to pink upon incubation at 37 °C. RGDS-fibres based on the A-, V- and S-spacer amphiphiles remained blue upon cell adhesion, which suggests that the packing in these fibres is too stable. The D-, N- and Q-fibre samples also remained blue, but this could be attributed to the diminished cell viability observed in these samples. The C-terminal amino acid has thus a great influence on the fibre ability to induce a colour change upon cell adhesion. Our data

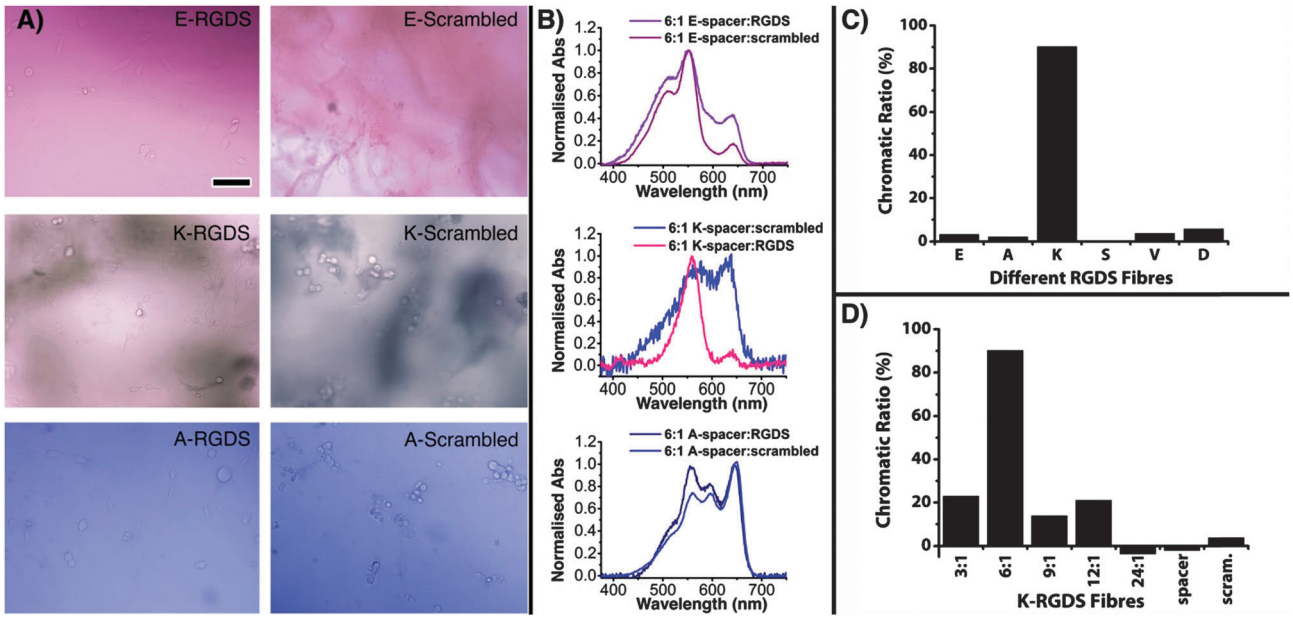

Fig. 3 (A) Brightfield widefield microscopy images of cell adhesion experiments and the corresponding UV-Vis absorption spectra. The colour captured by the brightfield camera is compared between the scrambled-fibres and the RGDS-fibres. Shown here are the results for the E-, K- and A-fibres. Because the E-fibres have the tendency to form large aggregates in the presence of cell culture medium, some of these superstructures can be observed in the E-scrambled sample. We did not observe similar aggregates for the K- and A-fibres. Scale bar represents 150 μm. (B) UV-Vis spectra recorded after the RGD-fibres and scrambled-fibres were incubated for 18 h in the presence of detached HeLa cells; a colour-shift from 630 nm to 550 nm is only observed for the K-RGDS fibres. (C) Chromatic ratios calculated for all the fibres that were suitable substrates for cell adhesion. (D) Chromatic ratios calculated for the K-RGDS fibres with a varying RGDS content.

suggests that an uncharged amino acid at the C-terminal position results in stable fibres that have no switching behaviour at physiologically relevant conditions. Incorporating an anionic residue however results in fibres that are too sensitive. Interestingly, only the cationic lysine yields functional fibres that are able to induce the desired colour change. For a schematic grouping of the C-terminal amino acids and a discussion on their propensity to induce a colour change upon cell adhesion see Fig. S2.7.1 (ESI†). For all fibres, the negative controls showed that HeLa cells were not able to adhere to any of the non-functionalised spacer-fibres, nor to the fibres with the scrambled domain. In these samples, only detached cells with a round morphology were observed.

To study the colour change caused by cell adherence to the fibres in more detail, UV-Vis spectra of the RGDS-fibres and scrambled fibres were recorded after incubation with detached HeLa cells for 18 h at 37 °C (Fig. 3B). The extent of the colour change was quantified by means of the chromatic ratio. The results are summarised in Fig. 3C and clearly show that the K-RGDS fibres displayed the largest colour change upon cell adhesion. These experiments were in full agreement with the brightfield microscopy experiments.

To investigate the influence of the fibre concentration on the cell adhesion properties and colour change upon cell binding, K-fibre solutions were also prepared at concentrations of 0.5 mg mL^{-1} and 0.75 mg mL^{-1} and were used to prepare samples for microscopy analysis as described above. We did not observe significant colour changes in the RGDS-containing samples and investigation by phase contrast microscopy revealed that for the 0.75 mg mL^{-1} fibre solutions about half of the observed cells remained detached while the rest of the population did adhere to the fibres. These conditions thus proved to be not sufficient to induce a similar colour change as observed for the sample prepared from a 1 mg mL^{-1} fibre solution. The amount of adherent cells was further diminished when a concentration of 0.5 mg mL^{-1} was used. Microscopy images for this experiment can be found in the ESI† (S2.6).

To investigate if the density of the RGDS motif present in the fibres had an effect on cell adhesion and thus the colour change, a collection of fibres was made in which the ratio of spacer amphiphile to RGDS amphiphile was varied from 3 : 1 to 24 : 1. Since only the K-fibres showed distinct colour-changing behaviour upon cell adhesion, we performed the RGDS-ratio studies only with the K-fibres. For this fibre series, both brightfield microscopy and UV-Vis spectroscopy experiments were performed as described above. These studies showed that a ratio of 6 : 1 spacer amphiphile to RGDS amphiphile gave the largest colour change, which was also reflected in the chromatic ratio calculated for this sample. Interestingly, increasing the RGDS content by making the 3 : 1 fibres, led to a less pronounced colour shift and importantly, only cells that were not spread were observed in this sample, suggesting that RGDS-content was in fact too high, inducing cytotoxicity. For the samples with a lower RGDS-content, the intensity of the colour change of the fibres decreased as the RGDS-content in the fibres was decreased from 6 : 1 to 24 : 1. These results are summarised by the chromatic ratios shown in Fig. 3D. For the 9 : 1 and 12 : 1 the brightfield microscopy showed that some

cells were still able to adhere to the fibres, although the amount of spread cells seemed to have decreased significantly with the reduced RGDS-content. Consequently the chromatic ratio was found to be much lower in these samples. Hardly any cell adhesion was observed for the sample with the lowest RGDS content, 24 : 1, and correspondingly no colour change was observed.

To investigate the cytotoxicity of the RGDS-containing fibres, live/dead assays based on calcein AM–ethidium homodimer-1 (EthD-1) were performed. The samples were prepared similarly to the procedure described above for the brightfield microscopy. After the incubation period, the cells were treated with calcein AM and EthD-1 and were analysed immediately by confocal laser scanning microscopy (CLSM). This experiment showed that cells adhering to the RGDS-fibres were viable and nicely spread. No significant differences in viability and cell count were observed among the various RGDS-fibres, with the exception of the previously mentioned N-, Q- and D-RGDS fibres. Furthermore, for all spacer- and scrambled-fibres, only cells with a round morphology were observed, however the viability of these cells varied with the incorporated spacer amphiphile. For example, for the E-fibres all observed cells in the negative controls were dead, whereas for the K-fibres the

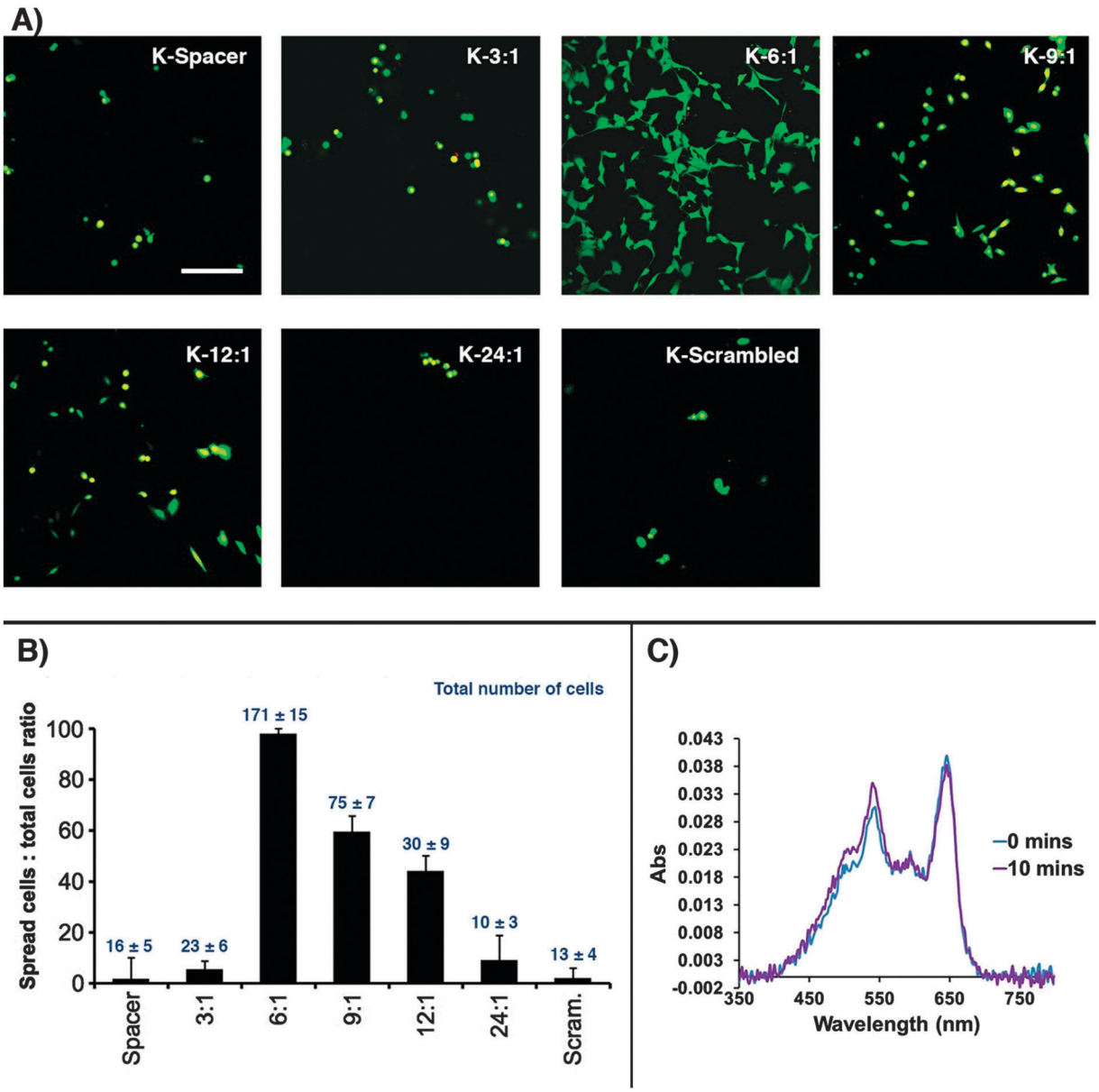

Fig. 4 (A) Cell viability images for the K-RGDS fibres and K-scrambled fibres. Images are composed from overlays of the calcein (green) and EthD-1 (red) signals. Scale bar represents 150 μm. (B) Data is composed out of 4 to 6 confocal microscopy images. Total amounts of cells are counted for each sample and shown in blue above the bars. The ratio between the amount of spread cells and total cell count was calculated and represented as the bars. A clear decrease in both cell count and the spread cells to total cells ratio is observed when the amount of RGDS in the fibres was lowered. (C) UV-Vis absorption spectra of the K-RGDS-fibres recorded after 0 and 10 minutes of incubation with the isolated human integrin protein. This shows a slight colour shift to pink after an incubation of 10 minutes.

cells were still viable, albeit not spread. Microscopy images for all other fibres can be found in the ESI† (S2.5). The series of K-RGDS-fibres with a gradual decreasing amount of RGDS were also studied using the live/dead assay (Fig. 4A). Our previous experiments using brightfield microscopy and UV-Vis spectrometry already suggested that HeLa cells could best adhere to the fibres made out of a 6 : 1 spacer-amphiphile to RGDS-amphiphile ratio, and the cell viability assay again confirmed that the 6 : 1 fibres are the best substrate for cell adhesion. The microscopy data from the cell viability experiment were used to quantify both the total amount of cells in each sample, and the amount of spread cells in each sample. It was found, as expected, that a ratio of 6 : 1 spacer amphiphile to RGDS amphiphile yielded the most optimal material for cell adhesion (Fig. 4B). Interestingly, increasing the RGDS content by making the 3 : 1 fibres, led to a large decrease in the total amount of cells, and importantly, only cells with a round morphology were observed in this sample. Furthermore, a gradual decrease in cell count and spread cells to total cells ratio was found when the RGD content was systematically lowered (Fig. 4B). This decrease correlates with the decrease in the chromatic ratio (Fig. 3D).

Integrin-mediated cell adhesion is induced by recognition of the RGD domain in the fibres by integrin receptors and this process is comprised of multiple events that can partially take place at the same time. Initially, cell attachment is induced by cell contact with the ECM that leads to ligand binding, allowing the cell to stick to a surface. Then, the cell starts to flatten and the cytoplasm will spread out over the substrate. This induces the organization of the actin cytoskeleton, after which focal adhesions will be formed that link the cytoskeleton to the ECM. Most probably, the colour change of the K-RGDS-fibres is induced during the first two steps of the cell adhesion process. To investigate whether cell attachment or cell spreading is most crucial for the colour-changing behaviour of the K-RGDS-fibres, UV-Vis experiments were performed in which the fibres were incubated with the isolated human $\alpha_V\beta_3$ integrin protein and followed in time for 10 minutes (Fig. 4C). During this experiment, a slight increase for the absorbance maximum at 550 nm was observed and a small decrease in the absorbance at 630 nm. This suggests that the initial cell binding to the fibres induces a small colour change, but that structural changes imposed on the diacetylene backbone by cell spreading are likely to be the most important step to set off the colour change. Interestingly, this mirrors the slight colour change observed for the 3 : 1 K-spacer : K-RGDS fibres for which it was found that cells could adhere to the surface, but were not able to spread (Fig. 3D and 4B). When the integrin binding experiment was performed using the stable A-RGDS-fibres, it was found that these fibres again remained blue.

Conclusions

In conclusion, polydiacetylene-containing peptide amphiphile fibres functionalised with the cell-binding moiety RGDS were designed to be able to detect the effect of cell adhesion on the chromatic properties of the polydiacetylene backbone. It was found that the K-RGDS fibres were most susceptible to a colour change, from blue to pink, induced by cell adhesion. RGDS containing fibres based on the spacer amphiphiles, V, A, S allowed the adhesion of viable cells, however, without undergoing a colour change. This may be due to the fact that the peptide components in these fibres have a more stable packing. The E-RGDS fibres were also a suitable substrate for cell adhesion, however these fibres were sensitive to the incubation temperature required for the cell studies, and thus turned pink upon incubation irrespective of cell adhesion. In contrast to this, the N-RGDS and Q-RGDS fibres were found to be cytotoxic to cells and the cell count was notably reduced in these samples. The D-RGDS fibres were also suboptimal for cell adhesion and a reduced cell count was observed in these samples. Furthermore, we were able to determine that a ratio of 6 : 1 K-spacer : RGDS was optimal for cell adhesion and consequently the biggest change in colour was observed for the K-RGDS fibres with this ratio. This suggests that the RGDS spacing in the fibres is an important factor in the degree of cell adhesion and spreading. Intriguingly, it was ascertained that the addition of the protein integrin could already trigger a slight colour change in the polydiacetylene backbone of the 6 : 1 K-RGDS fibres. Nonetheless, the steric crowding induced by cell spreading on the surface of the fibres is required to achieve a maximum colour change in the polydiacetylene backbone. In the future we would like to use this system to track cell migration both in 2D and 3D environments by incorporating our material in a suitable hydrogel. Furthermore, the sensing system presented here offers interesting possibilities as a screening method for cell culturing.

Acknowledgements

Elisabeth Pierson is acknowledged for helpful discussions, Kimberley Ghilarducci is thanked for contributions to the peptide synthesis. The department of General Instruments of the Radboud University Nijmegen is acknowledged for providing electron and light microscopy services. This work was financially supported by the Dutch Science Foundation (NWO, VICI and ECHO) and by the Ministry of Education, Culture and Science (Gravitation program 024.001.035).

Notes and references

1 X. Chen, Z. Zhou, X. Peng and J. Yoon, *Chem. Soc. Rev.*, 2012, **41**, 4610.
2 R. Jelinek and M. Ritenberg, *RSC Adv.*, 2013, **3**, 21192.
3 M. A. Reppy and B. A. Pinzola, *Chem. Commun.*, 2007, 4317.
4 G. Wegner, *Die Makromolekulare Chemie*, 1972, **154**, 35.
5 D. G. Rhodes, D. A. Frankel, T. Kuo and D. F. O'Brien, *Langmuir*, 1994, **10**, 267.
6 L. Hsu, G. L. Cvetanovich and S. I. Stupp, *J. Am. Chem. Soc.*, 2008, **130**, 3892.

7 E. Jahnke, I. Lieberwirth, N. Severin, J. P. Rabe and H. Frauenrath, *Angew. Chem., Int. Ed.*, 2006, **45**, 5383.
8 D. W. P. M. Löwik, I. O. Shklyarevskiy, L. Ruizendaal, P. C. M. Christianen, J. C. Maan and J. C. M. van Hest, *Adv. Mater.*, 2007, **19**, 1191.
9 M. A. Biesalski, A. Knaebel, R. Tu and M. Tirrell, *Biomaterials*, 2006, **27**, 1259.
10 D. Charych, J. Nagy, W. Spevak and M. Bednarski, *Science*, 1993, **261**, 585.
11 Q. Huo, S. Wang, A. Pisseloup, D. Verma and M. R. Leblanc, *Chem. Commun.*, 1999, 1601.
12 B. Hupfer, H. Ringsdorf and H. Schupp, *Chem. Phys. Lipids*, 1983, **33**, 355.
13 B. E. I. Ramakers, M. van den Heuvel, N. Tsichlis i Spithas, R. P. Brinkhuis, J. C. M. van Hest and D. W. P. M. Löwik, *Langmuir*, 2011, **28**, 2049.
14 A. Reichert, J. O. Nagy, W. Spevak and D. Charych, *J. Am. Chem. Soc.*, 1995, **117**, 829.
15 B. A. Pindzola, A. T. Nguyen and M. A. Reppy, *Chem. Commun.*, 2006, 906.
16 Z. Ma, J. Li, M. Liu, J. Cao, Z. Zou, J. Tu and L. Jiang, *J. Am. Chem. Soc.*, 1998, **120**, 12678.
17 Y. K. Jung, T. W. Kim, H. G. Park and H. T. Soh, *Adv. Funct. Mater.*, 2010, **20**, 3092.
18 M. P. Leal, M. Assali, I. Fernández and N. Khiar, *Chem. – Eur. J.*, 2011, **17**, 1828.
19 J. Deng, Z. Sheng, K. Zhou, M. Duan, C.-y. Yu and L. Jiang, *Bioconjugate Chem.*, 2009, **20**, 533.
20 Z. Orynbayeva, S. Kolusheva, E. Livneh, A. Lichtenshtein, I. Nathan and R. Jelinek, *Angew. Chem., Int. Ed.*, 2005, **44**, 1092.
21 E. Shtelman, A. Tomer, S. Kolusheva and R. Jelinek, *Anal. Biochem.*, 2006, **348**, 151.
22 M. van den Heuvel, D. W. P. M Löwik and J. C. M. van Hest, *Biomacromolecules*, 2008, **5**, 2727.
23 M. van den Heuvel, A. M. Prenen, J. C. Gielen, P. C. M. Christianen, D. J. Broer, D. W. P. M. Löwik and J. C. M. van Hest, *J. Am. Chem. Soc.*, 2009, **131**, 15014.
24 M. D. Pierschbacher and E. Ruoslahti, *Nature*, 1984, **309**, 30.
25 E. Ruoslahti and M. Pierschbacher, *Science*, 1987, **238**, 491.
26 U. Hersel, C. Dahmen and H. Kessler, *Biomaterials*, 2003, **24**, 4385.
27 C. M. Kolodziej, S. H. Kim, R. M. Broyer, S. S. Saxer, C. G. Decker and H. D. Maynard, *J. Am. Chem. Soc.*, 2011, **134**, 247.
28 S. F. M. van Dongen, P. Maiuri, E. Marie, C. Tribet and M. Piel, *Adv. Mater.*, 2013, **25**, 1687.
29 S. Tugulu, P. Silacci, N. Stergiopulos and H.-A. Klok, *Biomaterials*, 2007, **28**, 2536.
30 B. Trappmann, J. E. Gautrot, J. T. Connelly, D. G. T. Strange, Y. Li, M. L. Oyen, M. A. Cohen Stuart, H. Boehm, B. Li, V. Vogel, J. P. Spatz, F. M. Watt and W. T. S. Huck, *Nat. Mater.*, 2012, **11**, 642.
31 M. Mrksich, *Acta Biomater.*, 2009, **5**, 832.
32 K. A. Kilian and M. Mrksich, *Angew. Chem., Int. Ed.*, 2012, **51**, 4891.
33 E. Wischerhoff, K. Uhlig, A. Lankenau, H. G. Börner, A. Laschewsky, C. Duschl and J.-F. Lutz, *Angew. Chem., Int. Ed.*, 2008, **47**, 5666.
34 M. J. Webber, J. Tongers, M.-A. Renault, J. G. Roncalli, D. W. Losordo and S. I. Stupp, *Acta Biomater.*, 2010, **6**, 3.
35 E. Kaiser, R. L. Colescott, C. D. Bossinger and P. I. Cook, *Anal. Biochem.*, 1970, **34**, 595.
36 S. Keten, Z. Xu, B. Ihle and M. J. Buehler, *Nat. Mater.*, 2010, **9**, 359.
37 J. Zhang, R. Hao, L. Huang, J. Yao, X. Chen and Z. Shao, *Chem. Commun.*, 2011, **47**, 10296.
38 Z. Shao and F. Vollrath, *Nature*, 2002, **418**, 741.
39 M. van den Heuvel, N. van Gijzel, J. C. M. van Hest and D. W. P. M. Löwik, *Soft Matter*, 2015, **11**, 1335.
40 P. Y. Chou and G. D. Fasman, *Biochemistry*, 1974, **13**, 222.